OPTIMIZED PATH PLANNING FOR UAVS WITH AOA/SCAN BASED SENSORS

Kutluyıl Doğançay

School of Electrical and Information Engineering, University of South Australia
Mawson Lakes, SA 5095, Australia
Email: kutluyil.dogancay@unisa.edu.au

ABSTRACT

In emitter localization by unmanned aerial vehicles (UAVs) the objective of path planning is to determine the best UAV trajectories so as to maximize the instantaneous localization performance subject to various constraints. In this paper we propose gradient based waypoint update algorithms for UAVs equipped with angle-of-arrival (AOA) and scan based sensors. The optimization criterion used by the waypoint update algorithms is to maximize the determinant of the approximate Fisher information matrix. The effectiveness of the path planning algorithms is illustrated with several computer simulations.

1. INTRODUCTION

The objective of passive emitter localization is to determine the location of an emitter by processing the emitter signals received by several sensors or a moving sensor platform. Passive emitter localization finds application in mobile communications, wireless sensor networks and electronic warfare, to name but a few. The receiving platforms may employ sensors capable of measuring angle of arrival (AOA), time of arrival (TOA), time difference of arrival (TDOA), scan time, Doppler shift or received signal strength. Hybrid localization techniques combining some of these measurements are also available.

In this paper we consider optimal path planning for a particular type of receiving platform, namely unmanned aerial vehicles (UAVs) equipped with AOA and scan based sensors. The AOA localization has a rich history (see e.g. [1]). The key idea is to triangulate multiple bearing lines emanating from UAVs. The scan based localization exploits the geometric relationship between the emitter location and scan time measurements based on the assumption of constant beam rotation speed [2]. It is also related to rotating directional beacon techniques [3], [4] and landmark based robot localization techniques [5].

The approach adopted in this paper is to optimize UAV trajectories by locally maximizing the determinant of the approximate Fisher information matrix [6] each time a waypoint update is to be computed. This is equivalent to minimizing the estimation uncertainty. The Fisher information matrix is approximated by replacing the true emitter location with its maximum likelihood estimate [7]. The paper is organized as follows. Sections 2 and 3 provide an outline of the AOA and scan-based emitter localization problems. Section 4 discusses a hybrid localization technique involving both AOA and scan based sensors. Section 5 presents the hybrid maximum likelihood estimator for emitter location. In Section 6 the Fisher information matrix for scan-based localization is derived. Gradient-based UAV trajectory optimization techniques are developed in Section 7. Simulation results are presented in Section 8. The paper concludes in Section 9.

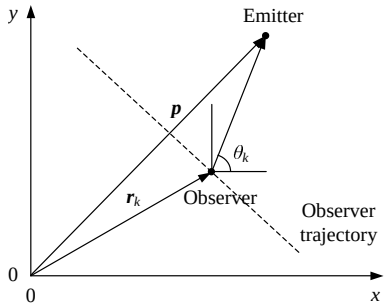

Figure 1: Two-dimensional bearings-only emitter localization from a single moving platform.

2. AOA LOCALIZATION

The two-dimensional passive emitter localization problem using AOA measurements is depicted in Fig. 1 where p is the location of a stationary emitter, and θ_k and r_k are the bearing angle and the sensor location, respectively, at time instant k. The relationship between the bearing angle, sensor location and emitter location is given by the following nonlinear equation:

$$\theta_k = \tan^{-1}\frac{\Delta y_k}{\Delta x_k}, \quad k = 1,\ldots,N \tag{1}$$

where $\Delta y_k = p_y - r_{y,k}$ and $\Delta x_k = p_x - r_{x,k}$. Here $p = [p_x, p_y]^T$ is the emitter location vector and $r_k = [r_{x,k}, r_{y,k}]^T$ is the sensor location at time instant k.

The objective of emitter localization is to estimate the emitter location p from a sequence of bearing measurements over the interval $1 \le k \le N$. In practice, the bearing measurements are corrupted by an additive noise, i.e.,

$$\tilde{\theta}_k = \theta_k + n_k \tag{2}$$

where the $\tilde{\theta}_k$, $k = 1,\ldots,N$, are the bearing measurements and n_k is the bearing noise. We assume that n_k is zero-mean i.i.d. Gaussian with variance σ_n^2. The bearing noise variance can vary with k.

3. SCAN BASED LOCALIZATION

The scan-based emitter localization algorithm [2] is an effective method for localizing scanning emitters such as a radar with a rotating beam. It exploits the constant scan rate of the radar antenna beam in order to derive geometric constraints on the emitter location. Fig. 2 depicts a scanning emitter in

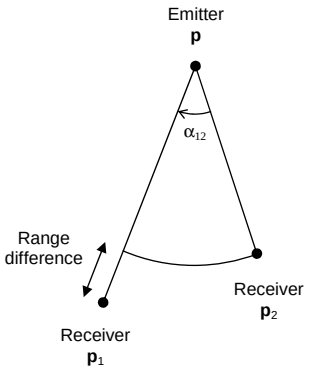

Figure 2: The subtended angle α_{12} depends on scan rate ω and TOI of the emitter beam at two receivers.

two-dimensional plane with scan rate (angular velocity) of ω rad/s and two receivers at locations p_1 and p_2 intercepting the emitter beam. Assuming prior knowledge of ω, the angle α_{12} subtended by the chord between the two receivers can be readily obtained from time of intercept (TOI) measurements of the emitter beam t_1 and t_2 at receivers p_1 and p_2, respectively,

$$\alpha_{12} = \omega|t_2 - t_1|. \quad (3)$$

The subtended angle is constrained to lie in the interval $[0, \pi]$ by ensuring that the emitter beam is intercepted during the shorter sweep time between the two receivers. The TOI measurements correspond to the peak location of the mainlobe of the emitter beam. Equation (3) ignores the additional time delay due to the range difference between the receivers $(\|p - p_1\|_2 - \|p - p_2\|_2)/c$ where $\|\cdot\|_2$ denotes the Euclidean norm and c is the speed of propagation for the emitter signal which is assumed to be $c = 3 \times 10^5$ km/s. In practice this time difference is negligible compared with $|t_2 - t_1|$ and is therefore ignored in the following development. Given α_{12} and the receiver locations p_1 and p_2, the loci of all possible emitter locations form a circular arc with centre point c_{12} and radius r_{12}:

$$c_{12}^{\pm} = \frac{p_1 + p_2}{2} + R_{12}^{\pm\pi/2} \frac{p_2 - p_1}{2\tan\alpha_{12}}, \quad r_{12} = \frac{\|p_2 - p_1\|_2}{2\sin\alpha_{12}} \quad (4)$$

where $R_{12}^{\pm\pi/2}$ is the $\pm 90^\circ$ rotation matrix

$$R_{12}^{\pm\pi/2} = \begin{bmatrix} 0 & \mp 1 \\ \pm 1 & 0 \end{bmatrix}. \quad (5)$$

This follows from a circle property that all angles subtended by a given chord are the same as long as they are on the same side of the chord (i.e., they remain either acute or obtuse). Only one of the circle centres $c_{12}^{\pm}$ corresponds to the true emitter location. The true circle centre can be determined from additional information such as angle of arrival or direction of beam rotation. We will denote the true circle centre by c_{12}.

4. AOA/SCAN BASED HYBRID LOCALIZATION

In hybrid localization UAVs are equipped with a heterogenous mix of sensors, thereby making a variety of sensor measurements available for localization purposes. In this paper AOA/scan based hybrid localization is considered. In

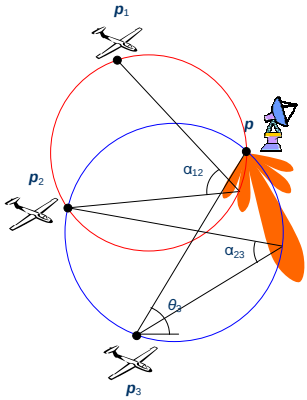

Figure 3: Hybrid localization with three UAVs. All three UAVs have scan time sensors and UAV3 has an additional AOA sensor.

AOA/scan based hybrid localization not all UAVs are required to have both AOA and scan based sensors. Some UAVs may only have one of these sensors. The use of hybrid sensors with an increased number of measurements in general leads to an improved overall localization performance. Fig. 3 depicts a geolocation scenario where all three UAVs have scan time sensors and UAV3 has an additional AOA sensor.

5. MAXIMUM LIKELIHOOD ESTIMATOR FOR HYBRID LOCALIZATION

AOA and scan time measurements can be modelled as Gaussian processes with joint conditional pdfs (likelihood functions) $f_{\text{AOA}}(\theta|p)$ and $f_{\text{SB}}(\alpha|p)$, respectively, where θ and α are AOA and subtended angle measurement vectors. The value of p that maximizes the likelihood function is the maximum likelihood estimate (MLE) of the emitter location:

$$\hat{p}_{\text{AOA}} = \arg\max_p f_{\text{AOA}}(\theta|p) \quad \hat{p}_{\text{SB}} = \arg\max_p f_{\text{SB}}(\alpha|p) \quad (6)$$

The maximization of log-likelihood (natural logarithm of likelihood function) reduces MLE to a nonlinear least-squares (NLS) problem:

$$\hat{p}_{\text{AOA}} = \arg\max_p e_{\text{AOA}}^T(p)\Sigma_{\text{AOA}}^{-1} e_{\text{AOA}}(p) \quad e_{\text{AOA}}(p) = \theta - \theta(p)$$
$$\hat{p}_{\text{SB}} = \arg\max_p e_{\text{SB}}^T(p)\Sigma_{\text{SB}}^{-1} e_{\text{SB}}(p) \quad e_{\text{SB}}(p) = \alpha - \alpha(p)$$

where Σ is the covariance matrix of the relevant sensor noise, and $\theta(p)$ and $\alpha(p)$ are exact AOA and subtended angles for an emitter at p. We note that the covariance matrix is dependent on the emitter range due to the link between the noise variance and SNR [7].

A hybrid MLE is easily formulated by augmenting the error vectors and corresponding covariance matrices in an appropriate manner. For example, if every UAV had AOA *and* scan based sensors, then the hybrid MLE combining all measurements would be given by

$$\hat{p}_{\text{H}} = \begin{bmatrix} e_{\text{AOA}}(p) \\ e_{\text{SB}}(p) \end{bmatrix}^T \begin{bmatrix} \Sigma_{\text{AOA}} & 0 \\ 0 & \Sigma_{\text{SB}} \end{bmatrix}^{-1} \begin{bmatrix} e_{\text{AOA}}(p) \\ e_{\text{SB}}(p) \end{bmatrix}. \quad (7)$$

For different sensor combinations the above hybrid estimator can be easily modified by removing relevant entries of the error vectors and the corresponding rows and columns of the covariance matrices.

6. FISHER INFORMATION MATRIX

The Cramer-Rao lower bound (CRLB) gives the smallest covariance matrix achievable by any unbiased estimator:

$$\text{CRLB} = \Phi^{-1}(p) \tag{8}$$

where $\Phi(p)$ is the Fisher information matrix (FIM)

$$\Phi(p) = E\left\{\left(\frac{\partial}{\partial p}\ln f(z|p)\right)\left(\frac{\partial}{\partial p}\ln f(z|p)\right)^T\right\}. \tag{9}$$

Here $f(z|p)$ is the log-likelihood function. Let J_o denote the Jacobian evaluated at the true emitter location p. FIM can then be expressed as

$$\Phi(p) = J_o^T \Sigma^{-1} J_o \tag{10}$$

where Σ is the covariance matrix of the single-sensor or hybrid-sensor measurement noise.

7. GRADIENT BASED WAYPOINT UPDATE ALGORITHMS

For an efficient estimator the area of 1-σ error ellipse (39.4% confidence region) $A_{1\sigma}$ is inversely proportional to the determinant of FIM:

$$A_{1\sigma} = \frac{\pi}{|\Phi(p)|^{1/2}}. \tag{11}$$

The path planning optimization criterion adopted in the paper is to minimize $A_{1\sigma}$ by adjusting the UAV waypoints. This is equivalent to *maximizing the determinant of FIM*. We note that the maximization of the determinant of FIM leads to the minimization of the localization uncertainty.

Let $s(k)$ be the 6×1 vector containing three UAV locations at an integer time index k:

$$s(k) = \begin{bmatrix} p_1(k) \\ p_2(k) \\ p_3(k) \end{bmatrix}. \tag{12}$$

The gradient descent algorithm

$$s(k+1) = s(k) + M(k)\frac{\partial J_T(s(k))}{\partial s(k)}, \quad k = 0,1,\ldots \tag{13}$$

produces waypoints for the UAVs by locally maximizing the determinant of an approximate FIM:

$$J_T(s(k)) = |\Phi(\hat{p}(k))| \tag{14}$$

where $\hat{p}(k)$ is MLE of the emitter location at time k. The step-size matrix $M(k)$ normalizes the waypoints so as to generate equal displacements for each UAV. This avoids UAVs closer to the emitter getting more favourable treatment and larger waypoints than other UAVs that are farther away from the emitter and also ensures constant velocity cruising for all UAVs. The gradient of the cost function in (13) can be numerically approximated by first-order finite differences [7].

The local optimization achieved by (13) is not always desirable especially if it leads to significantly long cruising times for UAVs. By compromising the initial performance a little one can achieve faster convergence on the emitter. To achieve this we introduce a "force" parameter β:

$$J_M(s(k)) = \frac{J_T(s(k))}{\sum_{i=1}^{3}\|p_i(k) - \hat{p}(k)\|^{\beta}}. \tag{15}$$

The smaller β the better the initial localization performance, and the larger β the faster the UAVs get to the emitter. The parameter β can be increased with k to improve overall performance. For $\beta = 0$, J_M and J_T are essentially identical.

In electronic warfare applications the UAVs may need to avoid certain geometric locations because of perceived threat. In optimized path planning soft constraints can be imposed on certain threat locations with a specified risk. The larger the risk associated with a threat the larger the desired UAV clearance will be. Circular soft constraints can be included in the cost function $J_M(s(k))$ as

$$J_c(s(k)) = J_M(s(k))\prod_{i=1}^{N_T}\prod_{j=1}^{3}\left(1 - e^{-\|p_j(k)-c_i\|/\kappa_i}\right) \tag{16}$$

where N_T is the number of threats, the c_i are the threat locations, and the $\kappa_i > 0$ are the threat intensities (risk associated with each threat). In (16) the multiplicative factors introduce global unstable minima at threat locations.

A certain minimum distance between the UAVs and the emitter must be maintained in order to maintain reception of the emitter signal due to vertical radar beamwidth. A hard constraint can be imposed on the geometry to realize this minimum clearance requirement. If the ith UAV reaches a distance $d_{\min}$ from the emitter, the hard constraint projects it onto a circle of radius $d_{\min}$ centred at the estimated emitter location:

$$p_i(k+1) = d_{\min}\frac{p_i(k+1) - \hat{p}(k)}{\|p_i(k+1) - \hat{p}(k)\|} + \hat{p}(k). \tag{17}$$

When all UAVs reach the hard constraint, they eventually attain the optimal angular separation minimizing MSE.

8. SIMULATIONS

Several simulations have been carried out to demonstrate the performance of the optimized path planning algorithms using three UAVs equipped with AOA and scan based sensors. The standard deviation of AOA sensors is 2.5° at a 50-km emitter range. The standard deviation of scan based measurements is 10 ms at 50 km. The UAVs cruise at a constant speed of 30 m/s. The emitters to be geolocated are at $[0,0]^T$ and $[-10,50]^T$ km (no prior knowledge of the emitter locations is available to the UAVs). Time separation between waypoint updates is 30 s. The parameter β is increased linearly from 0 to $\beta_{\max}$ during the geolocation mission for each emitter. The emitter scan rate is $\omega = \pi$ rad/s. The minimum allowed distance from the emitter is $d_{\min} = 5$ km. The initial UAV locations are $p_1(0) = [-45,25]^T$ km, $p_2(0) = [-42,30]^T$ km and $p_3(0) = [-44,33]^T$ km. There are two threats at $c_1 = [-19,18]^T$ km and $c_2 = [-25,2]^T$ km.

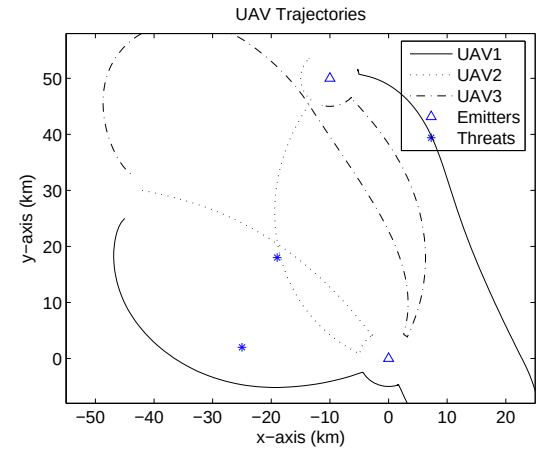

(a)

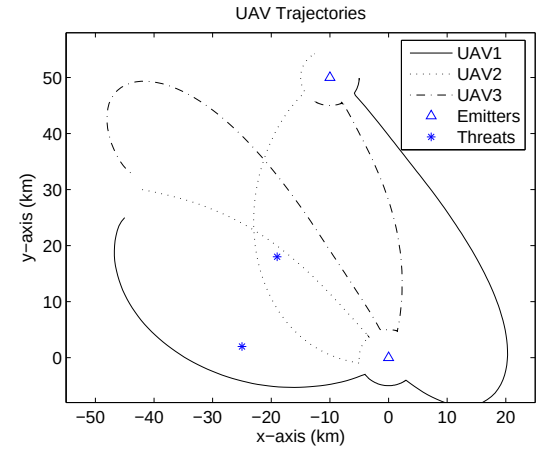

(b)

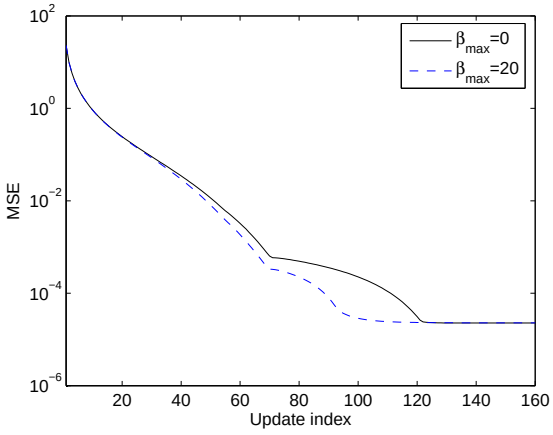

(c)

Figure 4: Optimized UAV paths when only scan time sensors are used and threats are ignored. (a) $\beta_{\max} = 0$, (b) $\beta_{\max} = 20$, and (c) the corresponding MSE plots for the first emitter.

Fig. 4 depicts the optimized UAV path trajectories when scan based sensors only are used and the threats are deemed to pose no risk. When $\beta_{\max} = 0$ the optimized trajectories exhibit strong baseline expansion initially and then form a closer formation as UAVs get close to the emitter. Increasing $\beta_{\max}$ to 20 not only reduces the initial baseline expansion, but also leads to faster convergence to the emitter by approximately 20 waypoints, which is equal to 10 min (see Fig. 4(c)).

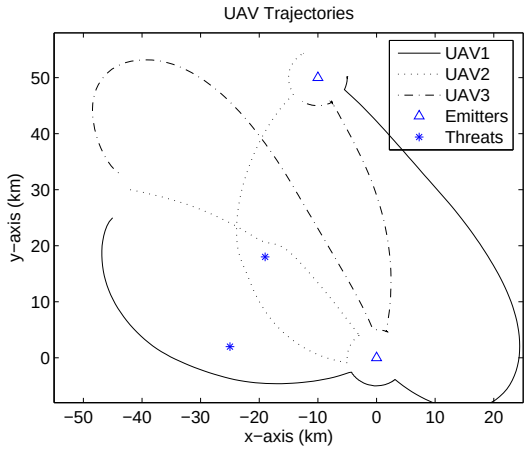

(a)

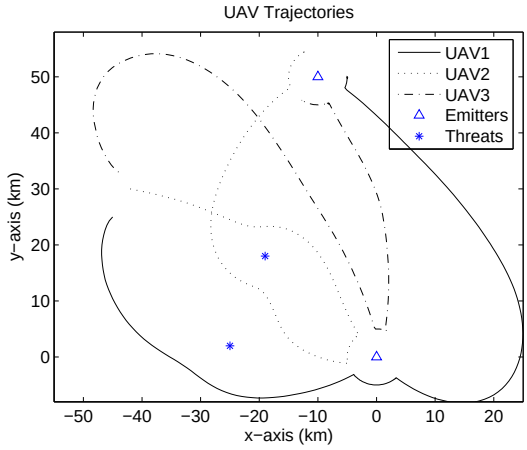

(b)

Figure 5: Optimized UAV paths (scan time sensors only) with soft constraints for $\beta_{\max} = 10$. (a) $\kappa_1 = \kappa_2 = 1$ and (b) $\kappa_1 = \kappa_2 = 5$.

The impact of soft constraints on the optimized trajectories for scan based sensors is shown in Fig. 5 for $\beta_{\max} = 10$. In Fig. 5(a) both threats have a risk of 1 ($\kappa_1 = \kappa_2 = 1$) whereas in Fig. 5(b) the risk of the threats is 5 ($\kappa_1 = \kappa_2 = 5$). The clearance of the threats by the UAVs is increased with larger κ_i.

The optimized trajectories for AOA sensors is shown in Fig. 6 for $\beta_{\max} = 10$. The threats have identical risks of 1 and 5 in Figs. 6(a) and 6(b), respectively. Note that the optimized trajectories for scan based and AOA sensors are markedly different. While for scan based localization the optimal angular separation between the three UAVs is 120° when they are equidistant from the emitter, the AOA localization is optimized if either 60° or 120° angular separation is achieved between the three UAVs [8]. In Fig. 6 we see that the UAVs eventually attain an angular separation of approximately 60° on the hard constraint.

The optimized trajectories for AOA/scan based hybrid sensors is demonstrated in Fig. 7 for two risk levels associated with the threats. Because the optimal angular separation of 120° is common to both AOA and scan based localiza-

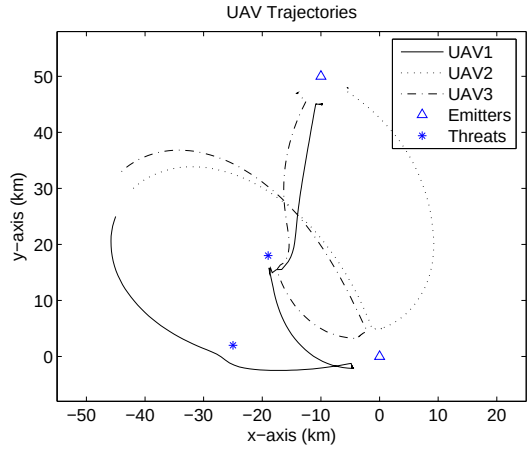

(a)

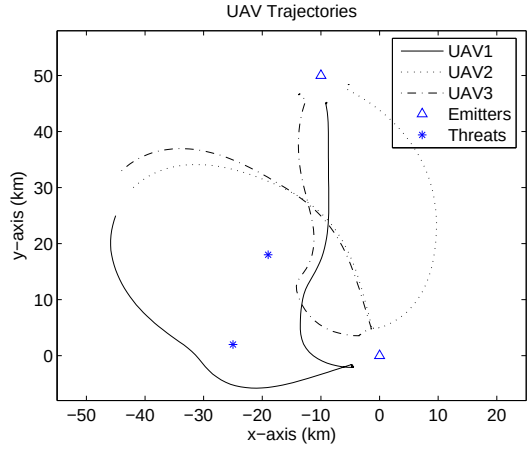

(b)

Figure 6: Optimized UAV paths (AOA sensors only) with soft constraints for $\beta_{\max} = 10$. (a) $\kappa_1 = \kappa_2 = 1$ and (b) $\kappa_1 = \kappa_2 = 5$.

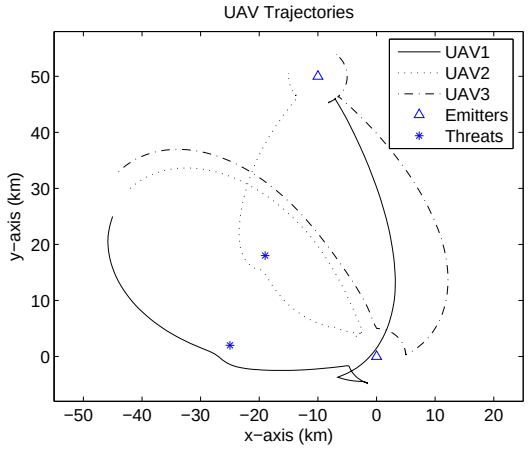

(a)

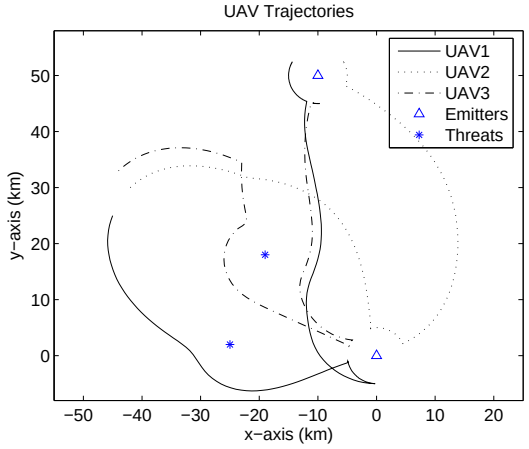

(b)

Figure 7: Optimized UAV paths (AOA/scan based sensors) with soft constraints for $\beta_{\max} = 10$. (a) $\kappa_1 = \kappa_2 = 1$ and (b) $\kappa_1 = \kappa_2 = 5$.

tion the final angular separation between the UAVs is roughly 120°.

9. CONCLUSION

This paper has presented optimal path planning algorithms for a triplet of UAVs equipped with AOA and scan based sensors. The use of different mixes of sensors results in markedly different optimized UAV paths. This emphasizes the need to account for different sensor characteristics. The proposed algorithms handle this requirement transparently without any human intervention to fine-tune the waypoint updates and, as an added bonus, do not necessitate prior knowledge of the emitter location.

REFERENCES

[1] S. C. Nardone and M. L. Graham, "A closed-form solution to bearings-only target motion analysis," *IEEE Journal of Oceanic Eng.*, vol. 22, no. 1, pp. 168–178, Jan. 1997.

[2] H. Hmam, "Scan-based emitter passive localization," *IEEE Trans. on Aerospace and Electronic Systems*, vol. 43, no. 1, Jan. 2007.

[3] C. D. McGillem and T. S. Rappaport, "A beacon navigation method for autonomous vehicles," *IEEE Trans. on Vehicular Technology*, vol. 38, no. 3, pp. 132–139, Aug. 1989.

[4] A. Nasipuri and K. Li, "A directionality based location discovery scheme for wireless sensor networks," in *Proc. First ACM Int. Workshop on Wireless Sensor Networks and Applications, WSNA 2002*, Atlanta, Georgia, Sep. 2002, pp. 105–111.

[5] I. Shimshoni, "On mobile robot localization from landmark bearings," *IEEE Trans. Robotics and Automation*, vol. 18, no. 6, pp. 971–976, Dec. 2002.

[6] Y. Oshman and P. Davidson, "Optimization of observer trajectories for bearings-only target localization," *IEEE Trans. on Aerospace and Electronic Systems*, vol. 35, no. 3, pp. 892–902, 1999.

[7] K. Doğançay, "Online optimization of receiver trajectories for scan-based emitter localization," *IEEE Trans. on Aerospace and Electronic Systems*, 2007, to appear.

[8] K. Doğançay and H. Hmam, "Optimal angular separation between receivers for AOA localization," *IEEE Trans. on Aerospace and Elect. Systems*, under review.